Available online at www.sciencedirect.com
SCIENCE DIRECT®
Journal of Solid State Chemistry 178 (2005) 3095–3100
JOURNAL OF SOLID STATE CHEMISTRY
www.elsevier.com/locate/jssc

A study of the NMR relaxation mechanisms of $ABCl_3$ (A = Rb, Cs, B = Cd, Mn) single crystals with the electric quadrupole and the electric magnetic types

Ae Ran Lim[a,*], Se-Young Jeong[b]

[a]*Department of Science Education, Jeonju University, Jeonju 560-759, Republic of Korea*
[b]*School of Nanoscience & Technology, Pusan National University, Pusan 609-735, Republic of Korea*

Received 4 June 2005; received in revised form 21 July 2005; accepted 26 July 2005
Available online 24 August 2005

Abstract

The ^{87}Rb and ^{133}Cs spin-lattice relaxation rates of $RbCdCl_3$ and $CsCdCl_3$ single crystals grown using the slow evaporation method were measured over the temperature range 160–400 K. The changes in the ^{87}Rb spin-lattice relaxation rate near 340, 363, and 395 K correspond to phase transitions of the $RbCdCl_3$ crystal. The jump in T_1^{-1} at 395 K is due to a shortening in the c-direction as a result of a phase transition from a cubic to a tetragonal structure. We suggest that the cubic Rb environment is favored above 395 K due to the fast motions and soft modes, which cause relaxation and average out the quadrupolar splittings. The temperature dependence of the relaxation rate below 340 K in $RbCdCl_3$ can be represented by $T_1^{-1} = \alpha T^2$ and is thus in accordance with a Raman process. The ^{133}Cs nuclei in the $CsCdCl_3$ crystal produce only one resonance line, which indicates that the local structure around the Cs atoms is cubic. The temperature dependence of the relaxation rate of the Cs nuclei can also be described with the quadratic equation $T_1^{-1} = \alpha T^2$. In the case of the $RbCdCl_3$ and $CsCdCl_3$ crystals, which are of electric quadrupolar type, their relaxations proceed via Raman processes, whereas in $RbMnCl_3$ and $CsMnCl_3$ crystals, which are of magnetic relaxation type, the relaxations proceed via single phonon processes. Therefore, the relaxation mechanisms of these different types of $ABCl_3$ crystals (quadrupolar and magnetic) are completely different NMR behavior.

Keywords: Physics of crystal growth; Nuclear magnetic resonance and relaxation; Phase transition; Ferroelectricity

1. Introduction

Many cubic perovskite crystals, $ABCl_3$ (A = Rb, Cs, B = Cd, Mn), undergo phase transitions to structures that are slightly distorted from ideal perovskite-type structures. $RbCdCl_3$ and $CsCdCl_3$ are among those $ABCl_3$ perovskite crystals that are acoustic-optic materials and thus of special interest for the study of phase transitions [1,2]. The $RbCdCl_3$ single crystal undergoes a first-order phase transition at $T_{c1} = 387.5$ K, a second-order phase transition at $T_{c2} = 363$ K, and a first-order phase transition at $T_{c3} = 339.5$ K [3]. From the high-temperature cubic phase (phase I), it transforms to a tetragonal phase (phase II) [3], then to an orthorhombic phase (phase III), and finally to another orthorhombic phase (phase IV). The $CsCdCl_3$ single crystal at room temperature is in the 6H polytype with a hexagonal perovskite structure [4], and does not exhibit any structural phase transitions in the temperature range 15–300 K [5]. These crystals have previously been investigated using electron paramagnetic resonance [6–10]. Their optical properties [11,12] and electrical conductivity [13] have also been studied. Although the physical properties of these materials have been reported, sufficient research has not yet been conducted

*Corresponding author. Fax: +82 (0) 63 220 2054.
E-mail addresses: aeranlim@hanmail.net, arlim@jj.ac.kr (A.R. Lim).

0022-4596/$ - see front matter © 2005 Elsevier Inc. All rights reserved.
doi:10.1016/j.jssc.2005.07.024

into their nuclear magnetic resonance (NMR) properties.

$RbMnCl_3$ and $CsMnCl_3$ crystals undergoes the paramagnetic to antiferromagnetic transitions at Neel temperatures, $T_N = 94.6$ and 67 K, respectively. We have recently measured the ^{87}Rb and ^{133}Cs spin-lattice relaxation rates in these crystals. In both crystals, the temperature dependencies of the relaxation rates for $T < T_N$ and $T > T_N$ were in accordance with a single-phonon process [14].

The comparison of $RbMnCl_3$ and $CsMnCl_3$ NMR measurements with those of $RbCdCl_3$ and $CsCdCl_3$ is of particular interest because these crystals are all $ABCl_3$-type crystals, and ^{87}Rb and ^{133}Cs NMR measurements for the $RbCdCl_3$ and $CsCdCl_3$ crystals have not previously been carried out.

The spin-lattice relaxation time of a nucleus is a measure of its dynamic properties such as its nucleus phonon interactions, and indicates how easily the excited state energy of the nuclear system is transferred to the lattice. In order to obtain detailed information about the dynamics of $RbCdCl_3$ and $CsCdCl_3$ crystals, it is thus useful to measure the spin-lattice relaxation times, T_1, of their ^{87}Rb and ^{133}Cs nuclei. The purpose of the current investigation is to study the nuclear spin-lattice relaxation rates, T_1^{-1}, of the ^{87}Rb and ^{133}Cs nuclei in $RbCdCl_3$ and $CsCdCl_3$ single crystals, respectively. These observations of the NMR characteristics of the ^{87}Rb and ^{133}Cs nuclei in these two similar crystals are new, so this work will enhance the understanding of their relaxation processes. These results are compared in this paper with those obtained for $RbMnCl_3$ and $CsMnCl_3$, which also belong to the family of $ABCl_3$ perovskite crystals.

2. Crystal structure

At room temperature, $RbCdCl_3$ single crystals have an orthorhombic structure with four molecules per unit cell, and belong to the space group $Pnma$ [15]. The lattice constants are $a = 8.962$ Å, $b = 4.034$ Å, and $c = 14.980$ Å at 293 K [16]. In this orthorhombic phase, each Cd atom is surrounded by six Cl atoms, which form a nearly regular octahedron.

Crystals of $CsCdCl_3$ at room temperature are in the 6H polytype with a hexagonal perovskite structure. The $CsCdCl_3$ crystal has a hexagonal structure and belongs to the space group $P6_3/mmc$. The cell parameters are $a = b = 7.418$ Å, $c = 18.39$ Å, and $Z = 6$ [17]. This crystal has two crystallographically distinct types of Cd ions occupying sites with D_{3d} and C_{3v} symmetries, denoted Cd(1) and Cd(2), respectively [18]. Both types of Cd atoms are surrounded by octahedra of Cl atoms.

3. Experimental method

The experiments were carried out using single crystals of $RbCdCl_3$ and $CsCdCl_3$ grown from aqueous solutions of RbCl and CsCl, respectively, with $CdCl_2$ in stoichiometric proportions by using slow evaporation at room temperature. The compounds always crystallized in the shape of thin rectangular parallelepipeds.

The NMR signals of ^{87}Rb and ^{133}Cs in the $RbCdCl_3$ and $CsCdCl_3$ single crystals were measured using the Bruker DSX 400 FT NMR spectrometer at the Korea Basic Science Institute. The static magnetic field was 9.4 T, and the central rf frequency was set at $\omega_0/2\pi = 130.93$ MHz for the ^{87}Rb nucleus and at $\omega_0/2\pi = 52.48$ MHz for the ^{133}Cs nucleus. The inversion recovery pulse sequence, $(\pi-\tau-\pi/2)$, was adapted, and the pulse widths and heights were selected so as to have enough frequency window when they are Fourier transformed into the frequency domain. The π pulse width and the pulse separation τ are 6.4 and 10 μs, respectively. The temperature-dependent NMR measurements were obtained over the temperature range 160–400 K. The sample temperatures were maintained at a constant value by controlling the helium gas flow and the heater current, providing a precision of ± 0.5 K.

4. Experimental results and analysis

We describe the recovery laws for the quadrupole and magnetic dipole–dipole relaxation process. For the quadrupole relaxation, the transition probability for $\Delta m = \pm 1$ as W_1 and that for $\Delta m = \pm 2$ as W_2 is shown in Fig. 1(a). Also, the recovery law in case of the dominant magnetic dipole–dipole relaxation is considered, and the transition probability is zero except for the transition $\Delta m = \pm 1$, as shown in Fig. 1(b), where it define as W.

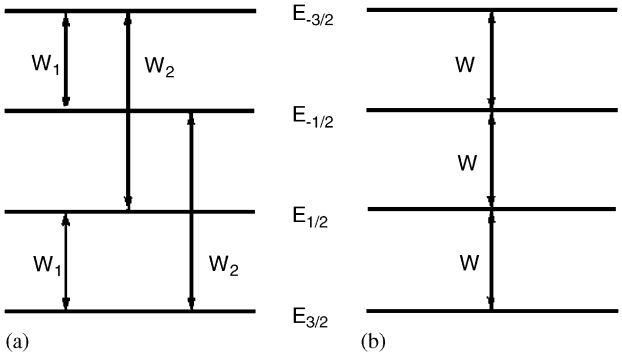

Fig. 1. Energy diagrams of the spin $I = 3/2$, and transition probability between them for the case of (a) quadrupole and (b) magnetic relaxation.

4.1. Spin-lattice relaxation times of ^{87}Rb in $RbCdCl_3$

The ^{87}Rb NMR spectrum has three resonance lines as a result of the quadrupole interactions of the ^{87}Rb ($I = \frac{3}{2}$) nucleus. When the crystal is rotated about the crystallographic axis, crystallographically equivalent nuclei give rise to three lines: one central line and two satellite lines. Usually, the quadrupole parameters of ^{87}Rb nuclei are large enough to be measured in MHz. Two satellite lines for the ^{87}Rb nucleus are far away from the central line. Therefore, the satellite lines are not easy to obtain. From our ^{87}Rb NMR result, four resonance lines are obtained in the range 190–390 K instead of three resonance lines. ^{87}Rb NMR spectrum at 300 K is shown in Fig. 2. The two groups of lines in this structure have different intensities. This result points to the existence of two types of crystallographically inequivalent ^{87}Rb nuclei, Rb(I) and Rb(II). The two central resonance lines correspond to chemically inequivalent sites, Rb(I) and Rb(II), and the other two resonance lines are caused by the ferroelastic domain structure. Above 395 K, only one resonance line is obtained for ^{87}Rb. This means that the structure above 395 K is cubic, i.e., of higher symmetry than the tetragonal structure.

The spin-lattice relaxation times of ^{87}Rb in $RbCdCl_3$ were measured over the temperature range 180–400 K. The recovery trace for the central line of ^{87}Rb ($I = 3/2$) with dominant quadrupole relaxation can be represented by a combination of two exponential functions [19–21]:

$$[S(\infty) - S(t)]/2S(\infty) = 0.5\exp(-2W_1t) + 0.5\exp(-2W_2t), \quad (1)$$

where W_1 and W_2 are the transition probabilities for $|\Delta m| = 1, 2$. Thus, the relaxation rates are given by

$$1/T_1 = 0.4(W_1 + 4W_2). \quad (2)$$

The variations with temperature of the spin-lattice relaxation rates for the four lines of Rb were measured. The recovery traces for the four resonance lines of ^{87}Rb with dominant quadrupole relaxation can be represented by a linear combination of two exponential functions (Eq. (1)). Fig. 3 shows the inversion recovery traces at 200, 320, and 400 K fitted with the two exponential functions. We measured the variation of the relaxation time of the resonance line for Rb with increasing temperature. The temperature dependence of the nuclear spin-lattice relaxation rate, T_1^{-1}, for ^{87}Rb is shown in Fig. 4. The variations of T_1^{-1} with temperature of the four resonance lines for Rb are very similar, and their values are the same within experimental error. The relaxation rate of the ^{87}Rb nucleus changes abruptly near 395 K. This discontinuity in the T_1^{-1} curve indicates that the phase I to phase II transition is a first-order transition. The jump in T_1^{-1} at T_{c1} is due to a shortening in the c-direction as a result of the phase transition from a cubic to a tetragonal structure. In phase I above 395 K

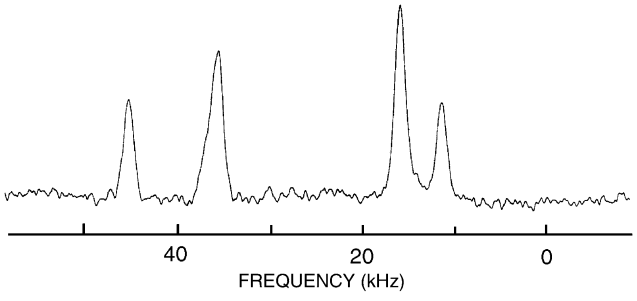

Fig. 2. NMR spectrum for Rb in $RbCdCl_3$ at room temperature.

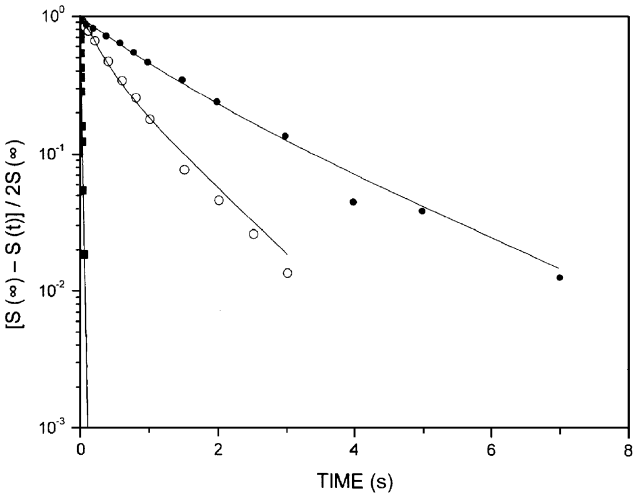

Fig. 3. Inversion recovery behavior of ^{87}Rb as a function of the delay time t at 200, 320, and 400 K (●: 200 K, ○: 320 K, and ■: 400 K).

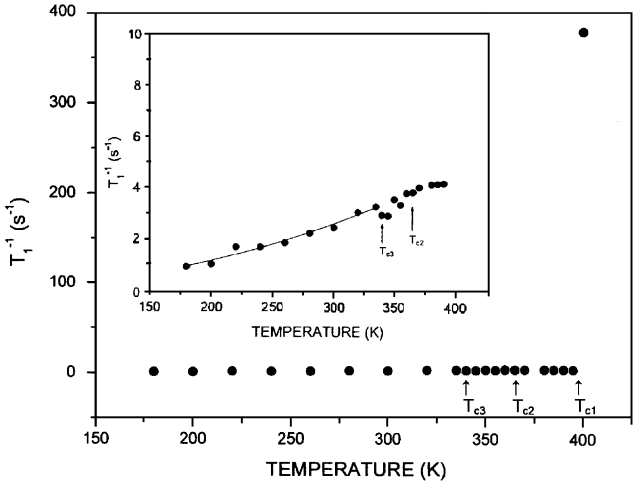

Fig. 4. Temperature dependence of the spin-lattice relaxation rates, T_1^{-1}, for Rb in a $RbCdCl_3$ crystal. The solid line is a fit using the function in Eq. (3).

($=T_{c1}$), the structure is cubic, and the spin-lattice relaxation time is 100 times faster than at 380 K; the cubic surroundings for Rb above 395 K due to the fast motions and soft modes, which cause relaxation and average out the quadrupolar splitting. The relaxation rate of the ^{87}Rb nucleus exhibits a change near 340 K ($=T_{c3}$), as shown in the inset of Fig. 4. The temperature dependence of T_1^{-1} near 363 K is more or less continuous, and is not affected by the phase III–II transition. The change in T_1^{-1} near 363 K ($=T_{c2}$) is very small, and the relaxation rate increases with increasing temperature in phases II, III, and IV. The T_1^{-1} data for Rb in phase IV (see the inset of Fig. 4) can be described with the following quadratic Eq. [22]:

$$T_1^{-1} = \alpha T_2, \tag{3}$$

where α is the constant, $3.0\times10^{-5}\,s^{-1}\,K^{-2}$, and T is the temperature. The spin-lattice relaxation rate can be fit by a T^2 dependence, and is consistent with a Raman process. The phonon processes affecting T_1^{-1} in phases II and III cannot be identified because of the narrow temperature ranges in which these phases are present.

4.2. Spin-lattice relaxation times of ^{133}Cs in $CsCdCl_3$

$CsCdCl_3$ with a hexagonal structure is expected to have a seven-line NMR spectrum due to the quadrupole interactions of ^{133}Cs ($I=\frac{7}{2}$). Instead of seven resonance lines, the ^{133}Cs nuclei in $CsCdCl_3$ produce only one resonance line in the temperature range 160–400 K, as shown in Fig. 5. This result indicates that the local structure around the Cs atoms is cubic.

The spin-lattice relaxation times of ^{133}Cs in $CsCdCl_3$ were measured by analyzing the inversion recovery sequence following the pulse. Since ^{133}Cs has a nuclear spin I of $\frac{7}{2}$, the most dominant relaxation mechanism in this temperature range is considered to be the fluctuation of the electric field gradient at the Cs site produced by Cl^- flips. In case with dominant quadrupole relaxation such as $CsCdCl_3$, the recovery trace for the central line of ^{133}Cs is not a single exponential type, but can be represented by a linear combination of four exponential functions. The signal for $W_1=W_2$ is given by [20,23,24]

$$\begin{aligned}[S(\infty)-S(t)]/2S(\infty) = {} & 0.048\ \exp(-0.476W_1t)\\ & +0.818\ \exp(-1.333W_1t)\\ & +0.050\ \exp(-2.381W_1t)\\ & +0.084\ \exp(-3.810W_1t),\end{aligned} \tag{4}$$

where $S(t)$ is the nuclear magnetization corresponding to the central transition at time t after saturation, and W_1 and W_2 are the transition probabilities corresponding to $\Delta m=\pm1$ and ±2, respectively. Again the return to equilibrium is characterized by four relaxation times but because of the much larger coefficient of the second exponential term, the growth is exponential in nature most of the time with relaxation rate equal to $1.333W_1$.

The temperature dependence of the nuclear spin-lattice relaxation rate, T_1^{-1}, of Cs is shown in Fig. 6. The spin-lattice relaxation times at 300 and 190 K are very long, 13 and 20 min, respectively. The relaxation rate, T_1^{-1}, increases with increasing temperature. The T_1^{-1} data for Cs in this temperature range can be described by $T_1^{-1}=(2.26\times10^{-9})T^2$, i.e. as a quadratic such as in Eq. (3). This means that the spin-lattice relaxation proceeds via a Raman process.

This result can be explained by the following relaxation mechanism: the lattice vibrations are coupled to the nuclear electric quadrupole moments by the dominant Raman processes (i.e., by absorption of one phonon ω and emission of another ω'). Here the frequencies ω and ω' of the two phonons satisfy the energy conservation relation $\omega-\omega'=\omega_0$ (where ω_0 is the nuclear Larmor frequency), so that all phonons inside the phonon spectrum contribute to the relaxation processes. The Raman-induced spin-lattice relaxation rate is then independent of the Larmor frequency. From the Debye approximation for the phonon

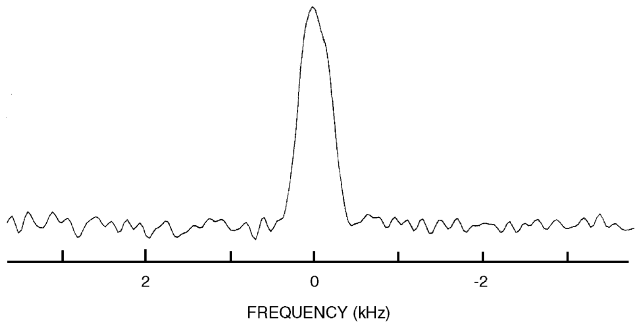

Fig. 5. NMR spectrum for Cs in $CsCdCl_3$ at room temperature.

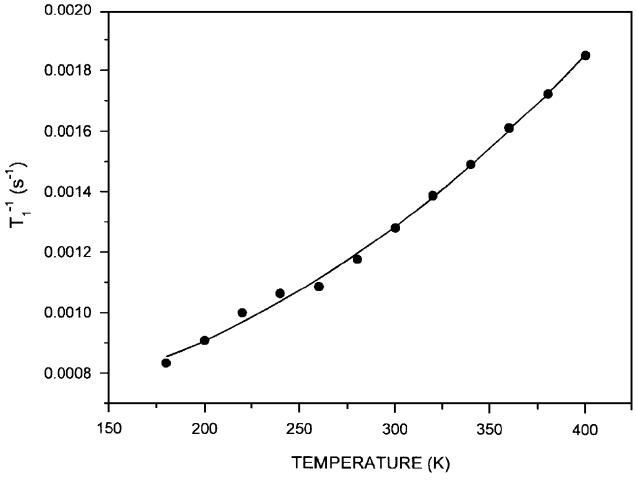

Fig. 6. Temperature dependence of the spin-lattice relaxation rates, T_1^{-1}, for Cs in a $CsCdCl_3$ crystal. The solid line is a fit using the function in Eq. (3).

density of states [25]

$$\left(\frac{1}{T_1}\right)_{\text{Raman}} = K\int_0^{\theta}\frac{\exp\{T'/T\}}{(\exp\{T'/T\}-1)^2}\left(\frac{T'}{\theta}\right)^6 dT', \qquad (5)$$

where θ is the Debye temperature. For $T \geqslant \theta$, $T_1^{-1} \propto T^2$, whereas at very low temperatures ($T/\theta \ll 0.02$), the temperature dependence is $T_1^{-1} \propto T^7$. Phonon-induced relaxation is commonly found in electron spin resonance spin-lattice relaxation [26] but is very rare in nuclear spin relaxation.

The temperature dependences of the spin-lattice relaxation rates, T_1^{-1}, of ^{87}Rb and ^{133}Cs in $RbCdCl_3$ and $CsCdCl_3$ crystals are proportional to the square of the temperature. Therefore, the nuclear spin-lattice relaxation processes in both crystals proceed via Raman processes.

5. Discussion and conclusions

The relaxation processes of the ^{87}Rb and ^{133}Cs nuclei in the $RbCdCl_3$ and $CsCdCl_3$ single crystals were studied over the temperature range 160–400 K. In the case of the $RbCdCl_3$ crystal, four resonance lines were obtained for phases II, III, and IV. Our results for phases II, III, and IV indicate that the two central resonance lines correspond to chemically inequivalent sites, Rb(I) and Rb(II), and that the other two resonance lines are caused by the ferroelastic domain structure. This result is supported by the two different quadrupole parameters previously reported for ^{87}Rb NMR in a phase III $RbCdCl_3$ crystal [27]. The recovery trace for the central line of ^{87}Rb can be represented by a linear combination of two exponential functions. The change in the spin-lattice relaxation rate near 395 K correspond to first-order phase transition in the crystal. The jump in T_1^{-1} at T_{c1} is due to a shortening in the c-direction as a result of the phase transition from the cubic to the tetragonal structure. We suggest that the cubic Rb environment is favored above 395 K due to the fast motions and soft modes, which cause relaxation and average out the quadrupolar splittings. The relaxation rate increases in phases II, III, and IV as the temperature increases. The temperature dependence in phase IV shown in Fig. 3 can be described with the quadratic equation $T_1^{-1} = \alpha T^2$. The temperature dependence of the relaxation rate in phase IV is in accord with a Raman relaxation process.

In $CsCdCl_3$ crystals, the ^{133}Cs nuclei produce only one resonance line instead of the expected seven resonance lines, which means that the local structure around the Cs atoms is cubic. The magnetization recovery of ^{133}Cs can be represented with a linear combination of four exponential functions. There are no abrupt changes in the relaxation rate with temperature, so there are no apparent phase transitions in this temperature range. The temperature dependence of the relaxation of the Cs nuclei in $CsCdCl_3$ can be described with $T_1^{-1} = \alpha T^2$, which is in accord with a Raman process.

We have compared the ^{87}Rb and ^{133}Cs NMR results obtained for the $RbCdCl_3$ and $CsCdCl_3$ crystals. The Cs relaxation time is about 200,000 times slower than the Rb relaxation time when both are in "cubic" surroundings at 400 K. Based on these results, the difference between the atomic weights of Rb and Cs is responsible for the differences between the spin-lattice relaxation rates in the $RbCdCl_3$ and $CsCdCl_3$ single crystals. The spin-lattice relaxations of the ^{87}Rb and ^{133}Cs nuclei in these crystals were shown to be due to Raman processes. Observations of Raman-induced spin-lattice relaxation ($T_1^{-1} = \alpha T^2$) have been observed in other system [28].

The NMR interaction mechanism in $RbCdCl_3$ and $CsCdCl_3$ is well known to be of the electric quadrupolar type whereas since $RbMnCl_3$ and $CsMnCl_3$ belong to the family of $ABCl_3$ crystals, the NMR relaxation mechanism in these crystals is presumably of magnetic origin. Therefore completely different NMR behavior is to be expected in these crystals, which is unlikely to be strictly related to their structural phase transitions. From our experimental results, $RbCdCl_3$ and $CsCdCl_3$ have relaxation mechanisms consisting of Raman processes, whereas the $RbMnCl_3$ and $CsMnCl_3$ crystals [28] undergo single phonon processes. The phase transition temperatures and the structures of the $ABCl_3$ (A = Rb, Cs, B = Cd, Mn) crystals are different each other, but their phase transition mechanisms are distinguished as the quadrupolar and magnetic origin. The differences between the chemical properties of Cd and Mn are expected to alter the nature of the phase transitions of these crystals. Therefore, the relaxation mechanism of these different types of $ABCl_3$ crystals (quadrupolar and magnetic) are completely different NMR behavior.

Acknowledgment

This work was supported by Grant No. R04-2003-000-10040-0 from the Basic Research Program of the Korea Science & Engineering Foundation.

References

[1] S. Melnikova, A. Anistratov, B. Beznosikov, Sov. Phys. Solid State 19 (1977) 1266.
[2] K.S. Alexandrov, A.T. Anistratov, S.V. Melnikova, V.I. Zinenko, L.A. Shabanova, B.V. Beznosikov, Ferroelectrics 20 (1978) 305.
[3] A.G. Ageev, A.N. Vtyurin, A.S. Krylov, A.D. Shefer, Crystallogr. Rep. 43 (1988) 58.

[4] E.A. Petrakovskaya, V.V. Velichko, I.M. Krygin, S.B. Petrov, L.G. Falaleeva, Sov. Phys. Solid State 25 (1983) 492.
[5] M.H. Kuok, J. Raman Spectrosc. 14 (1975) 264.
[6] G.L. McPherson, J.R. Chang, J. Magn. Reson. 14 (1974) 310.
[7] A. Edgar, J. Phys. C: Solid State Phys. 9 (1976) 4303.
[8] A.E. Usachev, Y.V. Yablokov, Sov. Phys. Solid State 22 (1980) 1253.
[9] M. Bensekrane, A. Goltzene, B. Meyer, C. Schwab, II Nuovo Cimento 2D (1983) 1964.
[10] W.C. Zheng, S.Y. Wu, Physica B 301 (2001) 186.
[11] S.V. Melnikova, A.T. Anistratov, B.V. Beznosikov, Sov. Phys. Solid State 19 (1977) 1266.
[12] M.C. Marco de Lucas, F. Rodriguez, H.U. Gudel, N. Furer, J. Lumin. 60&61 (1994) 581.
[13] M. Natarajan, E.A. Secco, Phys. Status Solidi A 33 (1976) 427.
[14] A.R. Lim, J.K. Jung, S.Y. Jeong, J. Appl. Phys. 91 (2002) 3095.
[15] M. Natarajan, H.E. Howard-Lock, I.D. Brown, Can. J. Chem. 56 (1978) 1192.
[16] F. Hamzaoui, I. Noiret, G. Odou, F. Danede, F. Baert, J. Solid State Chem. 124 (1996) 39.
[17] S. Siegel, E. Gebert, Acta Crystallogr. 17 (1964) 790.
[18] J.R. Chang, G.L. McPherson, J.L. Atwood, Inorg. Chem. 14 (1975) 3079.
[19] A. Avogadro, E. Cavelius, D. Muller, J. Petersson, Phys. Status Solidi B 44 (1971) 639.
[20] M.I. Gordon, M.J.R. Hoch, J. Phys. C: Solid State Phys. 11 (1978) 783.
[21] M. Igarashi, H. Kitagawa, S. Takahashi, R. Yoshizaki, Y. Abe, Z. Naturforsch. 47a (1992) 313.
[22] A. Abragam, The Principles of Nuclear Magnetism, Oxford University Press, Oxford, 1961.
[23] E.R. Andrew, D.P. Tunstall, Proc. Phys. Soc. (London) 78 (1961) 1.
[24] D.P. Tewara, G.S. Verma, Phys. Rev. 129 (1963) 1975.
[25] J. Dolinsek, U. Mikac, J.E. Javorsek, J.E. Lahajnar, R. Blinc, L.F. Kirpichnikova, Phys. Rev. B 58 (1998) 8445.
[26] B. Rakvin, N.S. Dalal, J. Phys. Chem. Solids 57 (1996) 1483.
[27] S. Plesko, R. Kind, J. Roos, J. Phys. Soc. Japan 45 (1978) 553.
[28] S. Chen, D.C. Ailion, Phys. Rev. B 40 (1989) 2332.